SIMPLE CONTROL LAWS FOR CONTINUOUS-THRUST ESCAPE OR CAPTURE AND THEIR USE IN OPTIMISATION

Anastassios E. Petropoulos,* Gregory J. Whiffen† and Jon A. Sims‡
Jet Propulsion Laboratory
California Institute of Technology
Pasadena, California 91109-8099

Interplanetary missions which use low-thrust, high specific impulse propulsion can further capitalise on the capabilities of the propulsion system by using it to effect escape from the launch body or capture at a target body. For multi-revolution escape or capture, where optimisation becomes increasingly laborious the larger the number of revolutions, we investigate simple control laws which not only offer reasonable estimates of the propellant-optimal performance, but also provide initial guesses for optimisation. We find that quite different control laws can often yield similar performance. The utility of these control laws as initial guesses for optimisation is also assessed.

Introduction

The problem of low-thrust escape from an initially circular orbit around a body with a $1/r^2$ gravity field has been studied by numerous researchers in the last few decades. In the late 1950s, Lawden[1,2] found that in the case of continuous, constant thrust acceleration, thrust in the tangential direction yields nearly the minimum characteristic velocity (and hence minimum propellant consumption and minimum escape time, assuming constant propellant mass flow rate).

In this paper we study the same problem, but with constant thrust and eccentric initial orbits, ultimately focusing on the geostationary transfer orbit (GTO). Using numerical integration of the equations of motion, we first determine the performance of tangential thrust over a wide range of initial eccentricities and periapse altitudes. Then, for the case of a nominal GTO initial orbit, we present four control laws for the thrust direction that out-perform the tangential-thrust law. The four laws have different functional forms which were selected from over fifteen functional forms that were studied in detail, each having its own set of parameters to adjust. The laws were selected based on their performance and on their perceived potential to serve in optimisation as initial guesses that might not only speed-up the optimisation process, but also lead to different local minima. We optimise each of these initial guesses, as well as the initial guess of tangential thrust, to achieve the minimum escape time. The optimisation software is based on the static/dynamic control (SDC) algorithm.[3–5] SDC best fits into the direct method category, although, unlike other direct methods, the explicit time dependence of the optimisation problem is not removed by parametrisation. We compare the number of iterations needed for convergence and the optimal solutions obtained from each initial guess.

In all numerical computations, the following parameters are assumed: The thrust is 465mN, the specific impulse is 3100s, the initial spacecraft mass is 1500kg, the radius of the central body (Earth) is 6378.14km, the gravitational parameter of the Earth is 398600.48504296km^3/s^2, and thrust commences at periapsis. The nominal GTO has a 200km periapsis altitude and an eccentricity of 0.7306. Shadowing is not considered.

Tangential Thrust Initial Guess

We examine the time needed to escape from initial Earth orbits of varying eccentricity, but of initial periapsis altitude fixed at 200km. For eccentricities near that of GTO, the escape time is found to oscillate significantly with initial eccentricity. This oscillation is depicted in Fig. 1, where the equations of motion are integrated using two approaches. The first approach uses the Runge-Kutta integrator of MATLAB, with the equations of motion expressed in polar coordinates and the thrust direction aligned with the velocity at each instant — that is, a continuously varying

*Senior Member of the Engineering Staff; Member AIAA; Member AAS.

†Senior Member of the Engineering Staff; Member AAS.

‡Senior Member of the Engineering Staff; Member AIAA; Member AAS.

Copyright © 2002 by Anastassios E. Petropoulos, Gregory J. Whiffen, and Jon A. Sims. Published by the American Institute of Aeronautics and Astronautics, Inc., with permission.

thrust direction. The second approach, which is also employed in the optimisation software, uses Cartesian coordinates to express the equations of motion, dividing the trajectory into a large number of management periods during each of which the thrust direction is inertially fixed. For tangential thrust, the inertial direction is that of the velocity vector at the start of the management period. The slight phase and upward shifts of the curve computed with the second approach are partly due to the higher integration accuracy used, and partly due to the stepped nature of the thrust direction.

The oscillation belies the effect of phasing. The local minima in escape time are all seen to occur for those initial orbits where the osculating eccentricity of the spiral trajectory almost reaches zero shortly before escape, subsequently increasing roughly linearly with time to unity. In effect, "escape occurs from apoapsis," that is, at the point when the spacecraft has nearly reached the last apoapsis before escape, enough thrust is available to circularise the orbit, effectively turning apoapsis to periapsis and continuing with a positive and increasing flight path angle up to escape. Whether the correct timing is obtained to effect these conditions depends on the initial orbit, since the thrust and gravitational parameters are assumed fixed.

The amplitude of the oscillations is greater, the greater the eccentricity. The local minima and maxima may be thought of as providing an envelope for the escape times. Fig. 2 shows these envelopes for various initial periapsis altitudes and initial eccentricities varying from zero to about 0.85. As expected, the oscillations are of zero amplitude at zero eccentricity, and grow steadily with increasing eccentricity. The envelopes were produced with the Runge-Kutta integrator.

The nominal GTO orbit was deliberately chosen to provide an escape time near a local maximum for the tangential thrust control law (using the stepped-thrust integrator). With this orbit and thrust law, we try to tax the optimisation process as much as possible, in a sense obtaining an upper bound on the difficulty of the optimisation.

Having established the nominal initial orbit, we may instead adjust the thrust control law to obtain the correct phasing for escape from apoapsis. We now present four control laws which accomplish this.

Control Laws

In developing the control laws, two basic approaches are taken. The first is a simple trial and error approach, where the thrust angle is assumed to be of a certain functional form, with parameters in the functions serving as secondary controls that determine the precise thrust angle. The second approach, which might be termed a "guided trial and error approach," involves maximising weighted averages of the rates of change of the osculating orbital elements. The exact weightings, or functional forms of the weightings, then become the secondary controls. This approach has been taken in the past, for example, by Kluever[6] and Gefert.[7] Thrust along the velocity vector, which maximises the rate of increase of orbital energy (or, equivalently, semimajor axis), is the simplest example of this approach.

The thrust direction is specified in terms of the thrust angle, α, which is measured from the circumferential direction, positive away from the gravitational centre (as for the flight path angle, γ). Three of the more successful trial-and-error functional forms for α, with numerical parameters tailored for the nominal GTO, are given by

$$\alpha_{f11} = \gamma\left(1+\mathrm{e}^{-n}-\mathrm{e}^{n(|\theta/\pi|-1)}\right)^{\mathrm{e}^{-[rv^2/(2\mu)]}}, \quad \text{with } n=2 \tag{1}$$

$$\alpha_{f46} = \gamma - m|\sin\gamma|(\sin^2\gamma)^{\mathrm{e}^{n[rv^2/(2\mu)]}}, \quad \text{with } m=35.75,\ n=5 \tag{2}$$

$$\alpha_{f50} = \gamma_{(\theta+\phi)}, \quad \text{with } \phi=8^\circ \tag{3}$$

where $\theta \in (-\pi, \pi]$ is the osculating true anomaly, r is the radius, v is the velocity, and μ is the gravitational parameter of the central body. It is evident that these three equations provide variations from the tangential thrust law, $\alpha = \gamma$. In the last equation, for example, $\gamma_{(\theta+\phi)}$ represents a simple phase shift which gives the thrust angle as the flight path angle not at the current position, but on the osculating conic at a true anomaly advanced by ϕ from the current osculating true anomaly. The tailoring of the numerical parameters was based on escape time computed with the same integrator used by the optimisation program.

An examination of the escape spiral for each of the control laws given by Eqs. 1–3 reveals that the escape from apoapsis characteristic is present in each case. With this observation in mind, we develop a thrust law based on maximising the rate of decrease of the impulsive ΔV needed to escape from the osculating apoapsis radius. The thrust angle giving the maximal rate of decrease is found using the variational equations for the semi-major axis, a, and the eccentricity, e, along with elementary conic relations. A weighting factor, c_w, is included for added flexibility. The value $c_w = 1$ gives the maximal rate. An adjustment away

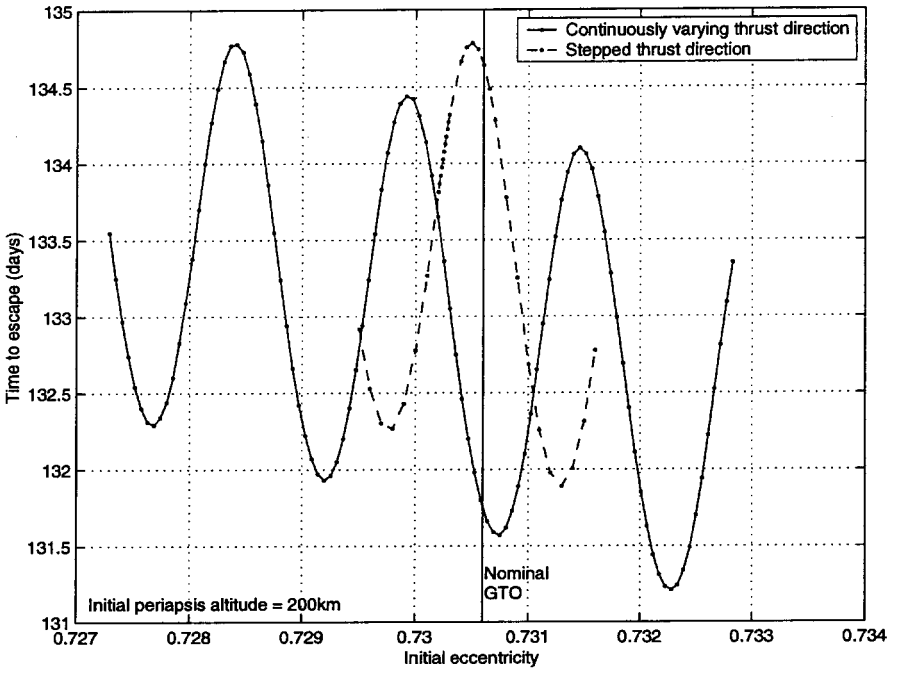

Fig. 1 Oscillation in escape time using tangential thrust for various initial Earth orbits, with thrust starting at periapsis.

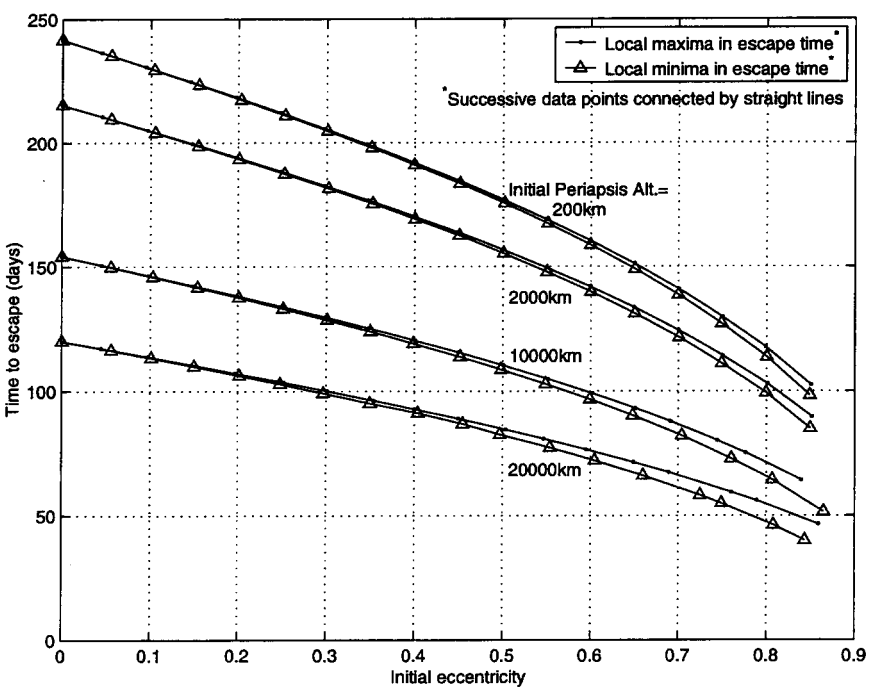

Fig. 2 Upper and lower bounds in escape time using tangential thrust for various initial Earth orbits, with thrust starting at periapsis.

from unity will typically be needed to give the minimum escape time. The thrust angle, then, is given by:

$$\alpha_{f56} = \gamma - \frac{\pi}{2} - \mathrm{atan}(c_w c_t, c_{no}) \tag{4}$$

where

$$\begin{aligned} c_t &= \frac{av}{\sqrt{r_a \mu}}\left(\sqrt{1-e} - \sqrt{2}\right) \\ &\quad + \frac{e+\cos\theta}{v}\sqrt{\frac{\mu}{r_a}}\left[\frac{2-\sqrt{2(1-e)}}{(1+e)\sqrt{1-e}}\right] \end{aligned} \tag{5}$$

$$c_{no} = \frac{r\sin\theta}{2av}\sqrt{\frac{\mu}{r_a}}\left[\frac{2-\sqrt{2(1-e)}}{(1+e)\sqrt{1-e}}\right] \tag{6}$$

with r_a representing the osculating apoapsis radius, $r_a = a(1+e)$. The notation $\phi = \mathrm{atan}(y, x)$ is shorthand for ($R\sin\phi = y$, $R\cos\phi = x$). For the nominal GTO, the weighting coefficient is set to $c_w = 2.8$ to obtain a favourable escape time.

To again illustrate the phasing issue, the four control laws of Eqs. 1–4, and the tangential thrust law (designated α_{f1}), are applied to orbits near the nominal GTO. The escape times, using the stepped-thrust integrator, are shown graphically in Fig. 3. Except for α_{f1}, the other thrust laws are close to their minimum escape time when the nominal GTO (eccentricity 0.7306) is the initial orbit. The thrust angles are shown graphically in Fig. 4 for the initial and final portions of the spiral trajectory.

Optimisation

Starting in the nominal GTO, the SDC optimiser is used to minimise the escape time, with five different initial guesses which are obtained by integrating the four control laws of Eqs. 1–4 and the tangential thrust law. Approximately 60 management periods, during each of which the thrust direction is held inertially fixed, are used per revolution. The optimisation involves 18729 independent variables.

Data for the initial guesses and corresponding optimised solutions are compared in Table 1, which shows the number of revolutions and time required for escape, the difference in escape time between the initial guess and optimal solution, and the number of iterations needed for convergence. It is evident from the table that there are two distinct local minima in escape time, that from the tangential thrust law, α_{f1}, and that from each of the other initial guess control laws. The first and lower minimum has about $93\frac{1}{4}$ revolutions, while the second and slightly higher minimum has about $94\frac{1}{4}$ revolutions. The difference in the fourth decimal place of the escape time for the α_{f11}-based optimum when compared with the subsequently-listed solutions in Table 1 is attributable to slight differences in the precision to which the convergence criteria are met, rather than to the presence of a different local minimum. The number of iterations for the α_{f56} solution is considerably less than the number needed by the other initial guesses leading to the same optimum because of the experience gained in selecting parameters that control the optimisation. The computation time needed for the optimisation of the α_{f56} initial guess was about 8.4 hours on a SunBlade 1000 workstation.

Both of the optimal solutions retain from the initial guesses the number of integral revolutions required for escape. In the α_{f1} case, the optimisation reduced the number of revolutions by almost a half, and also obtained the escape from apoapsis condition (absent from the initial guess), as seen in the optimal flight-path-angle and thrust-angle profiles depicted in Fig. 5. The optimal thrust direction is seen to lie close to the velocity vector except near the maxima and minima in flight-path angle. From the thrust-angle profile we see that as the spiral progresses, the apoapsis direction does not change significantly except on the last revolution. Thus, the last apoapsis would be expected to fall at about 92.5 revolutions, but because enough thrust is available, the apoapsis is pushed forward and the flight-path angle remains very close to zero for about $\frac{1}{4}$ revolution, the nadir occurring about $\frac{1}{4}$ revolution after the 92.5-revolution mark (see Fig. 5). (Were the nadir exactly at zero, then the apoapsis and periapsis points would have coalesced into one, this being the basis for the term "escape from apoapsis.") From its last nadir, the flight-path angle rises increasingly fast with polar angle up to escape, that is, $\mathrm{d}^2\gamma/\mathrm{d}\theta^2$ is greater than zero. From the last nadir about half a revolution remains before escape. Thus, escape occurs about $\frac{3}{4}$ revolutions after crossing the approximate direction of all but the last apoapses. The spiral trajectory is depicted in Fig. 7, with the departure direction seen to be about $\frac{1}{4}$ revolution past the initial periapsis.

The second locally optimal solution, whose flight-path-angle and thrust-angle profiles are shown in Fig. 6, also has the escape from apoapsis condition, although it occurs almost exactly one revolution later than in the first optimal solution. The optimisation did not significantly alter the number of revolutions of the initial guesses leading to the second optimum. Furthermore, the initial guesses also exhibited the escape from apoapsis condition. Indeed, it would appear that the optimisation strove to retain this characteristic. Rather than reducing flight time by a gradual reduction in the revolutions to escape,

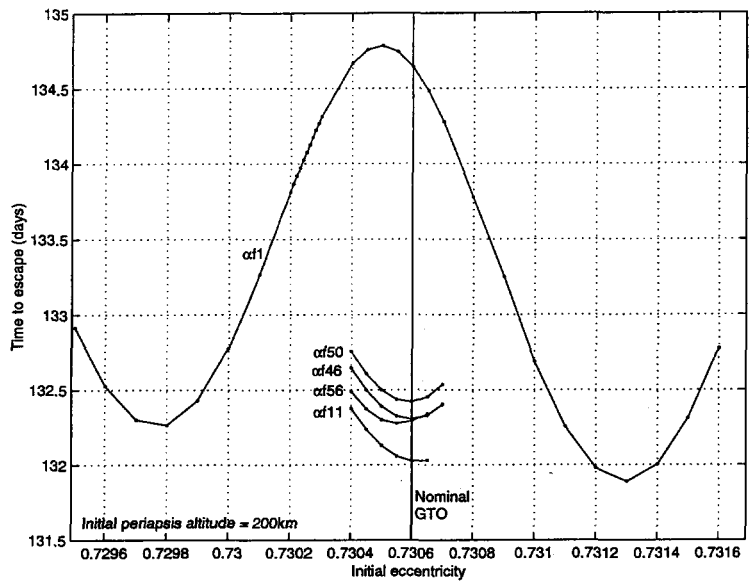

Fig. 3 Variation in escape time for various thrust profiles and various initial orbits near the nominal GTO. Integrations performed with the stepped-thrust integrator.

Table 1 Comparison of empirical and time-optimised escape from the nominal GTO

Init. Guess Control Law	Init. Guess Revs.	Opt. Esc. Revs.	Init. Guess Esc. Time (days)	Opt. Esc. Time (days)	Diff. (days)	Iterations
α_{f1}	93.683	93.296	134.6423	131.1838	3.4585	4685
α_{f11}	94.284	94.258	132.0265	131.4582	0.5683	2771
α_{f46}	94.284	94.258	132.3053	131.4584	0.8469	3740
α_{f50}	94.258	94.258	132.4205	131.4584	0.9621	3974
α_{f56}	94.226	94.258	132.2921	131.4584	0.8337	1631[a]

[a]Significantly lower than for other control laws because of experience gained in selecting parameters that control the optimisation.

which would have necessitated giving up escape from apoapsis, the optimiser chose to adjust significantly the thrust profile over the first few revolutions so as to minimise the time spent in the initial phases of the spiral, compared to the initial guess. This indicates that the presence of the escape from apoapsis condition is highly desirable. Given the fact that the two optima differ by about one full revolution, it is further noteworthy that the difference in flight time is only 0.2746 days, or 0.6248 times the orbital period of the initial GTO orbit. The spiral trajectory of the second optimum is shown in Fig. 8, graphically demonstrating that the escape direction is similar to that of the first optimum (Fig. 7).

Conclusions

Widely differing thrust histories can provide comparable, good performance in the problem of minimum-time, multi-revolution, constant-thrust escape or capture. Emprically-derived control laws have few parameters, or even just one, that can be adjusted to give close-to-optimal performance and provide good initial guesses for optimisation. For escape from eccentric initial orbits, the optimisation process favours the presence of an "escape from apoapsis" condition, wherein enough thrust is available to circularise the orbit when the final apoapsis is reached, escaping shortly thereafter.

For the specific case of escape from geostationary transfer orbit, two local minima in flight time were found, differing only slightly in escape time, but the longer one taking almost exactly one full revolution more to escape and exhibiting a markedly different thrust angle. In evaluating different initial guesses, rather than selecting the guess with the minimum escape time, it may be more important to select the one with the smallest number of full revolutions in

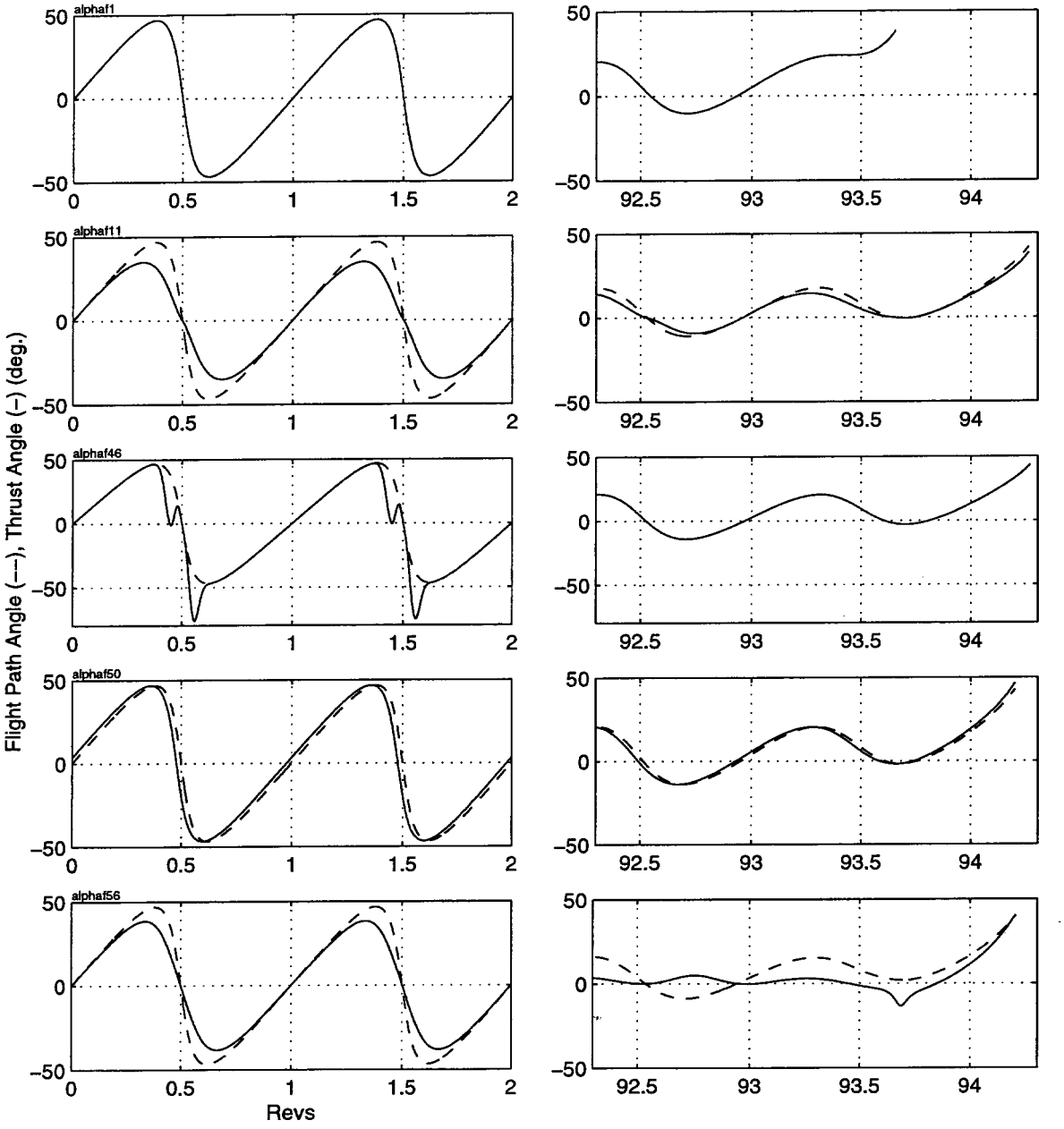

Fig. 4 Thrust profiles and flight-path angles of five different initial guesses for escape from GTO. The dashed curve for the flight-path angle is invisible in some cases due to superimposition on the solid curve.

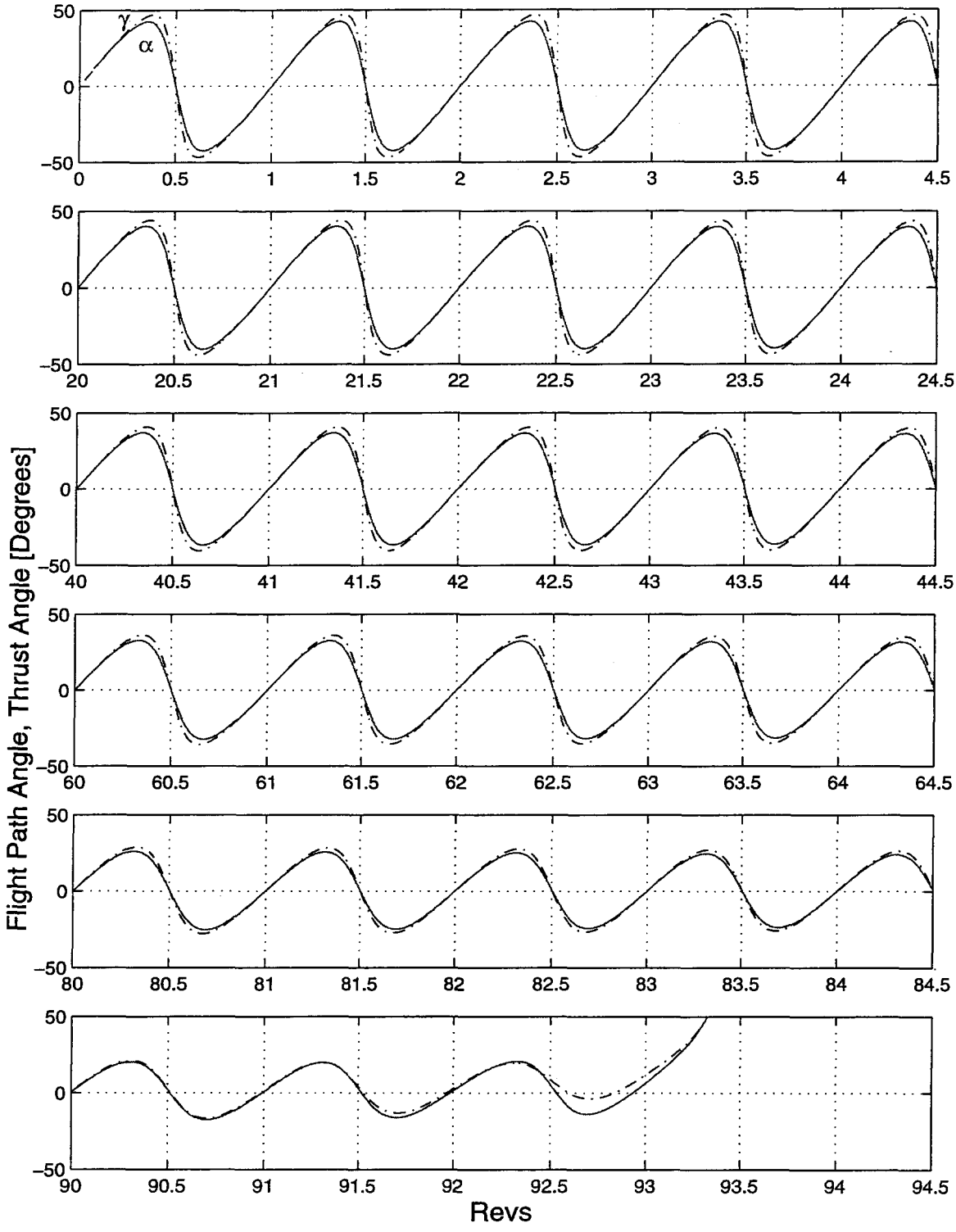

Fig. 5 Thrust profile for time-optimised escape from GTO, using SDC with an initial guess of tangential thrust (α_{f1}). This is the lower of two local optima.

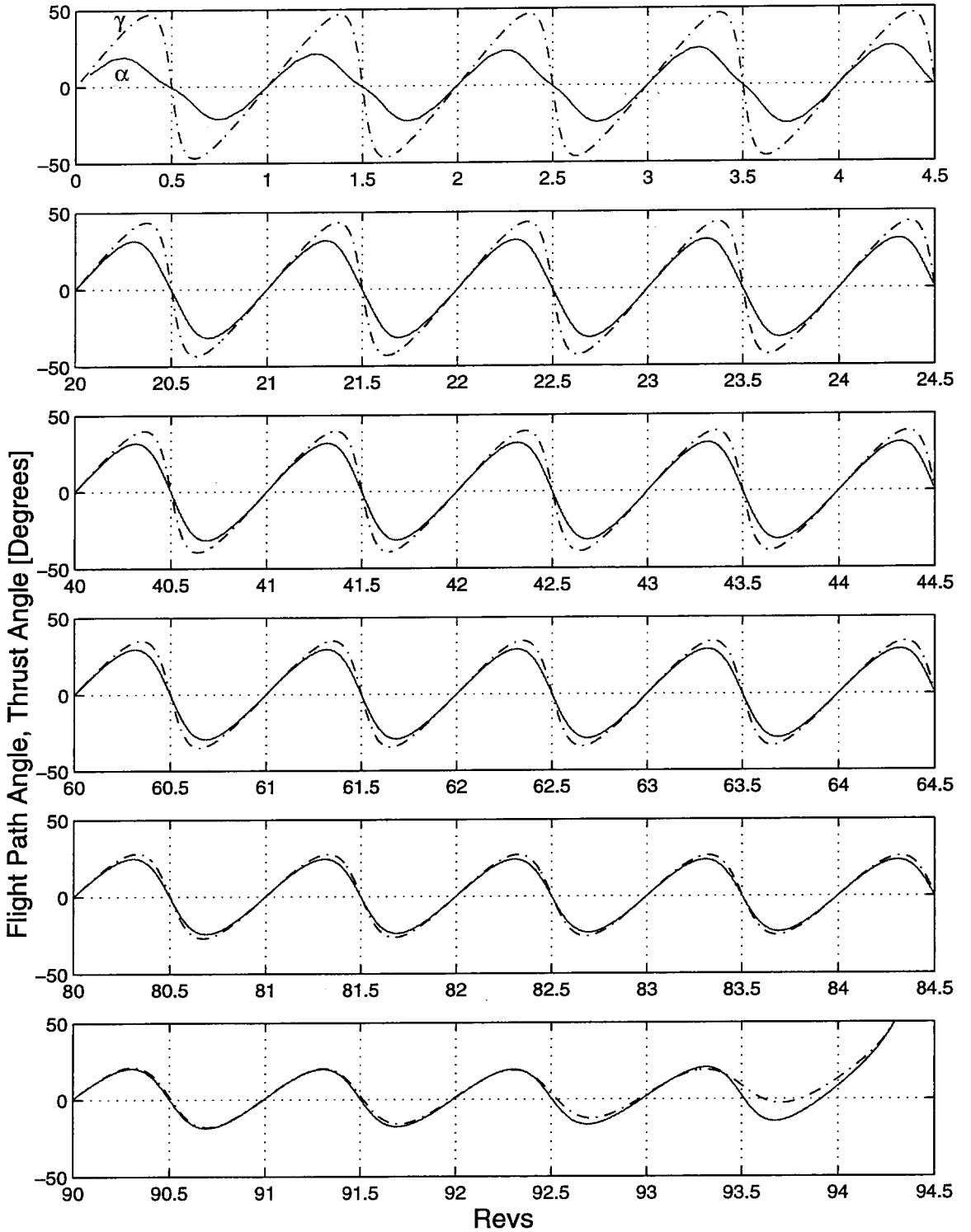

Fig. 6 Thrust profile for time-optimised escape from GTO, using SDC with an initial guess of α_{f46}. This is the higher of two local optima, attained also with the initial guesses α_{f11}, α_{f50}, and α_{f56}.

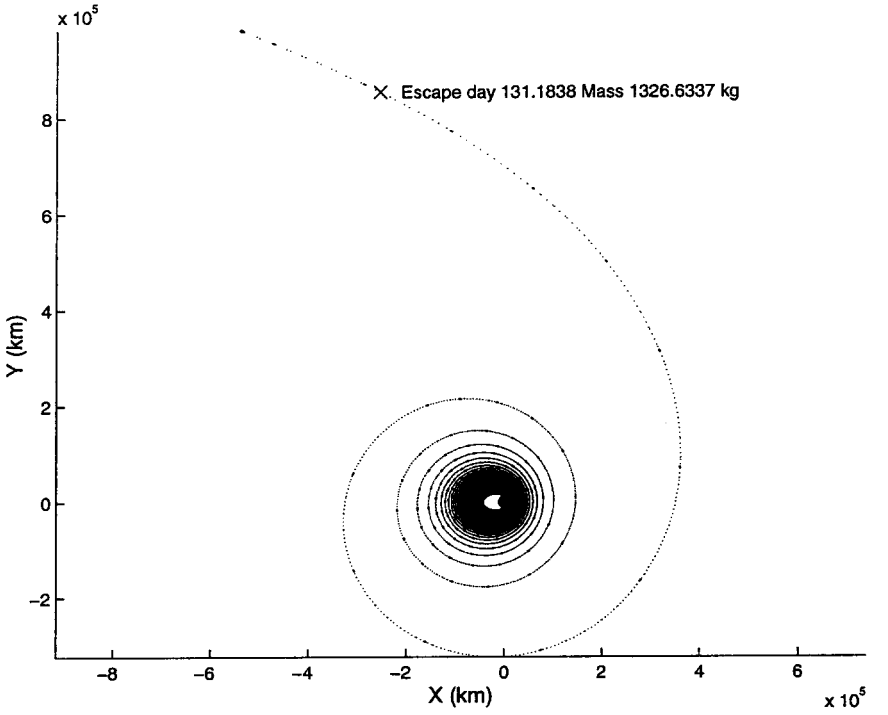

Fig. 7 Spiral trajectory for time-optimised escape from GTO, using SDC with an initial guess of tangential thrust (α_{f1}). This is the lower of two local optima.

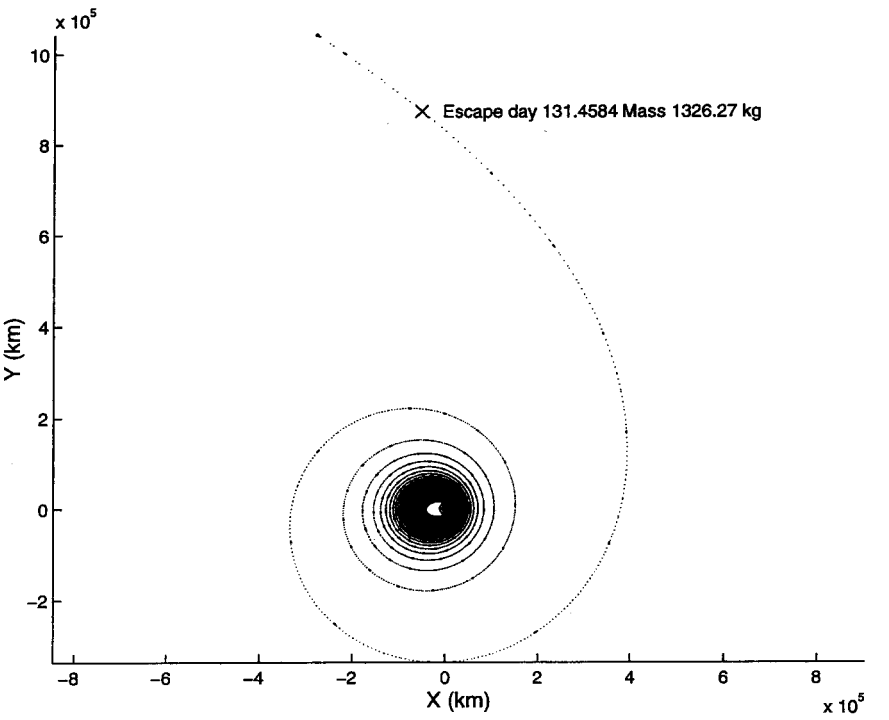

Fig. 8 Spiral trajectory for time-optimised escape from GTO, using SDC with an initial guess of α_{f46}. This is the higher of two local optima, attained also with the initial guesses α_{f11}, α_{f50}, and α_{f56}.

order to find with optimisation the lowest of possibly many local minima. However, the further away from the optimum the escape time of the initial guess, the longer the optimisation is likely to take.

It would be worth further investigating the optimisation time needed by other low-revolution initial guesses. Furthermore, while it would be of academic interest to find local minima with larger number of revolutions, it would certainly be useful to find the lower limit on the number of revolutions required to escape. It would also be of interest to investigate the applicability of the escape from apoapsis condition to other spiral escape problems, such as fixed-time, minimum-propellant transfers, where the thrust need not be continuous.

Acknowledgements

This research was carried out at the Jet Propulsion Laboratory, California Institute of Technology, under a contract with the National Aeronautics and Space Administration.

References

[1]Lawden, D. F., "Optimal Programming of Rocket Thrust Direction," *Astronautica Acta,* Vol.1, 1955, pp.41–56.

[2]Lawden, D. F., "Optimal Escape from a Circular Orbit," *Astronautica Acta,* Vol.4, 1958, pp.218–233.

[3]Whiffen, G. J. and Sims, J. A., "Application of a Novel Optimal Control Algorithm to Low-Thrust Trajectory Optimization," AAS/AIAA Space Flight Mechanics Meeting, AAS Paper 01-209, Santa Barbara, California, Feb. 11-15, 2001.

[4]Whiffen, G. J. and Sims, J. A., "Application of the SDC Optimal Control Algorithm to Low-Thrust Escape and Capture Trajectory Optimization," AAS/AIAA Space Flight Mechanics Meeting, AAS Paper 02-208, San Antonio, Texas, Jan. 27-30, 2002.

[5]Whiffen, G. J. and Sims, J. A., "Application of the SDC Optimal Control Algorithm to Low-Thrust Escape and Capture Including Fourth-Body Effects," Proceedings of the 2nd International Symposium on Low Thrust Trajectories, Toulouse, France, June 18-20, 2002.

[6]Kluever, C. A., "Simple Guidance Scheme for Low-Thrust Orbit Transfers," *J. Guidance, Control, and Dynamics,* Vol.21, No.6, Nov. 1998, pp.1015–1017.

[7]Gefert, L. P. and Hack, K. J., "Low-Thrust Control Law Development for Transfer from Low Earth Orbits to High Energy Elliptical Parking Orbits," AAS/AIAA Astrodynamics Specialist Conference, AAS Paper 99-410, Girdwood, Alaska, Aug. 1999.